

# Silicon Micromachined 400-600-GHz Orthomode Transducer

Zahraa Rizk<sup>1\*</sup>, Christopher Moore<sup>1</sup>, Michael E. Cyberey<sup>1</sup>, Arthur W. Lichtenberger<sup>1</sup>, Robert M. Weikle<sup>1</sup>, and N. Scott Barker<sup>1</sup>

**Abstract**— This paper presents the design, fabrication, and performance of a silicon-micromachined orthomode transducer (OMT) that operates in the 400-600 GHz band (WR-1.9 band). The simulation results show an insertion loss of 0.5 dB, a return loss >10 dB, isolation >35 dB and a cross polarization >35 dB over 85% of the frequency band.

**Keywords**— Orthomode transducer, silicon micromachined, ICP-CVD, THz.

## I. INTRODUCTION

**T**ERAHERTZ systems are becoming increasingly important in many fields such as astronomy [1,2], astrophysics spectroscopy [3], remote sensing, communication [4], and security applications [5,6].

Orthomode transducer (OMT) is a three-port passive device that has been used in receivers to discriminate between two orthogonal polarizations in the receiving antenna within the same frequency band [7]. At high frequencies, fabricating OMTs using the traditional metal machining becomes a challenge because of the small dimensions which require high precision and uniformity. Silicon micromachining is also more advantageous than CNC machining since entire batches of complex devices can be fabricated with lower costs and less time.

A multi-step deep reactive ion etching (DRIE)-based silicon micromachining is used to fabricate the OMT shown in Fig.1 [8]. The OMT consists of seven steps of different depths ranging from 22  $\mu\text{m}$  to 284  $\mu\text{m}$ . To obtain the stepped-shape structure in the Si, our fabrication process involves depositing  $\text{SiO}_2$  masks with different step thicknesses that are proportional to the Si step depths. The  $\text{SiO}_2$  layers are deposited using Inductively Coupled Plasma Chemical Vapor Deposition (ICP-CVD) technique which results in good surface uniformity ( $\pm 5$  nm) compared to other deposition methods. Next, we run the Bosch process so that the  $\text{SiO}_2$  layers and the Si are etched cumulatively until the whole  $\text{SiO}_2$  is etched and the Si features are obtained. The Si step depths are measured using an optical profilometer. Finally, gold electroless plating is used to make the surface conductive.

## II. RESULTS

The simulation results of the OMT design presented in Fig.1 show a return loss better than 10 dB over 85% of the bandwidth for both vertical and horizontal polarizations as shown in Fig.2. Moreover, the insertion loss and the cross-polarization level are

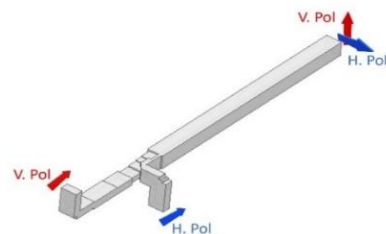


**Fig.1.** Three- dimensional OMT design and polarizations. V. Pol: Vertical polarization, H. Pol: Horizontal polarization.

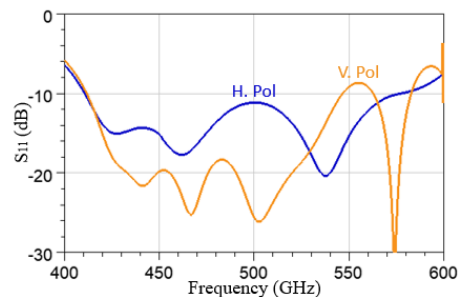


**Fig. 2.** Simulated S11 at the output ports of the OMT.

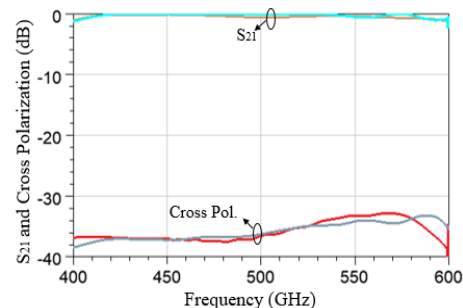


**Fig.3.** Simulated S<sub>21</sub> and cross polarization of the OMT.

demonstrated in Fig.3 where the insertion loss is less than 0.7 dB, and the cross polarization is better than 35 dB over the 85% of the frequency range. Additionally, the port isolation is

<sup>1</sup>Electrical and Computer Engineering Department, University of Virginia, Charlottesville, 22904, USA. \*Zahraa Rizk (email: zar8z@virginia.edu).

better than 30 dB over the whole range.

Additional simulations with step depths tolerance of  $\pm 5 \mu\text{m}$  showed similar results with a return loss better than 10 dB over 80% of the bandwidth for both vertical and horizontal polarizations, insertion loss less than 1 dB, and a cross polarization better than 29 dB over the whole frequency band as shown in figures 4 and 5 respectively.

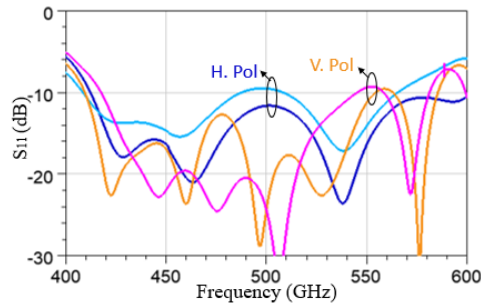


**Fig. 4.** Simulated  $S_{11}$  at the output ports of the OMT with step depths tolerance of  $\pm 5 \mu\text{m}$ .

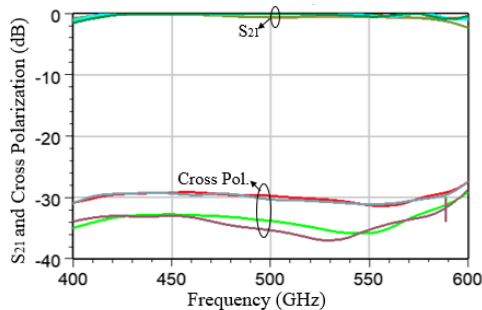


**Fig.5.** Simulated  $S_{21}$  and cross polarization of the OMT with step depths tolerance of  $\pm 5 \mu\text{m}$ .

## REFERENCES

- [1] H.W. Hubers, R. Eichholz, S. G. Pavlov and H. Richter, "High Resolution Terahertz Spectroscopy with Quantum Cascade Lasers", *Journal of Infrared, Millimeter, and Terahertz Waves* 34(5) pp. 325-341, 2013.
- [2] C. Kulesa, "Terahertz Spectroscopy for Astronomy: From Comets to Cosmology," *IEEE Transactions on Terahertz Science and Technology*, 1(1), pp.232-240, 2011.
- [3] S. Withington, "Terahertz Astronomical Telescopes and Instrumentation," *Philosophical Transactions of the Royal Society of London. Series A: Mathematical, Physical and Engineering Sciences*, 362(1815), pp.395-402, 2004.
- [4] P. Rodríguez-Vázquez, J. Grzyb, N. Sarmah, B. Heinemann and U.R. Pfeiffer, "A 65 Gbps QPSK One Meter Wireless Link Operating at a 225-255 GHz Tunable Carrier in a SiGe HBT Technology," *In 2018 IEEE Radio and Wireless Symposium (RWS)*, pp.146-149, January, 2018.

- [5] K.B. Cooper, R.J. Dengler, N. Llombart, B. Thomas, G. Chattopadhyay and P.H. Siegel, "THz Imaging Radar for Standoff Personnel Screening," *IEEE transactions on terahertz science and technology*, 1(1), pp.169-182, 2011.
- [6] H. Quast, and T. Löffler, "Towards Real-Time Active THz Range Imaging for Security Applications," *In 2009 International Conference on Electromagnetics in Advanced Applications*, pp. 501-504, IEEE, September, 2009
- [7] A. Navarrini, C. Groppi, and G. Chattopadhyay, "A Waveguide Orthomode Transducer for 385-500 GHz," *In 21st International Symposium on Space Terahertz Technology 2010, ISSTT 2010*, pp. 281-290, December, 2010.
- [8] C. Jung-Kubiak, T.J. Reck, J.V. Siles, R. Lin, C. Lee, J. Gill, K. Cooper, I. Mehdi and G. Chattopadhyay, "A multistep DRIE process for complex terahertz waveguide components," *IEEE Transactions on Terahertz Science and Technology*, 6(5), pp. 690-695, 2016.

## NOTES: